Publications from USDA-ARS / UNL Faculty

U.S. Department of Agriculture: Agricultural Research Service, Lincoln, Nebraska

2017

Identification of Novel Seroreactive Antigens in Johne's Disease Cattle by Using the Mycobacterium tuberculosis Protein Array

John Bannantine

Joseph J. Campo

Lingling Li

Arlo Randall

Jozelyn Pablo

See next page for additional authors

Follow this and additional works at: https://digitalcommons.unl.edu/usdaarsfacpub

Part of the Agriculture Commons

Authors

John Bannantine, Joseph J. Campo, Lingling Li, Arlo Randall, Jozelyn Pablo, Craig A. Praul, Juan Antonio Raygoza Garay, Judith R. Stabel, and Vivek Kapur

Clinical and Vaccine Immunology®

Identification of Novel Seroreactive Antigens in Johne's Disease Cattle by Using the *Mycobacterium tuberculosis* Protein Array

John P. Bannantine,[a] Joseph J. Campo,[b] Lingling Li,[c] Arlo Randall,[b] Jozelyn Pablo,[b] Craig A. Praul,[c] Juan Antonio Raygoza Garay,[c] Judith R. Stabel,[a] Vivek Kapur[c]

U.S. Department of Agriculture, Agricultural Research Service, National Animal Disease Center, Ames, Iowa, USA[a]; Antigen Discovery, Inc., Irvine, California, USA[b]; Pennsylvania State University, University Park, Pennsylvania, USA[c]

ABSTRACT Johne's disease, a chronic gastrointestinal inflammatory disease caused by *Mycobacterium avium* subspecies *paratuberculosis*, is endemic in dairy cattle and other ruminants worldwide and remains a challenge to diagnose using traditional serological methods. Given the close phylogenetic relationship between *M. avium* subsp. *paratuberculosis* and the human pathogen *Mycobacterium tuberculosis*, here, we applied a whole-proteome *M. tuberculosis* protein array to identify seroreactive and diagnostic *M. avium* subsp. *paratuberculosis* antigens. A genome-scale pairwise analysis of amino acid identity levels between orthologous proteins in *M. avium* subsp. *paratuberculosis* and *M. tuberculosis* showed an average of 62% identity, with more than half the orthologous proteins sharing >75% identity. Analysis of the *M. tuberculosis* protein array probed with sera from *M. avium* subsp. *paratuberculosis*-infected cattle showed antibody binding to 729 *M. tuberculosis* proteins, with 58% of them having ≥70% identity to *M. avium* subsp. *paratuberculosis* orthologs. The results showed that only 4 of the top 40 seroreactive *M. tuberculosis* antigens were orthologs of previously reported *M. avium* subsp. *paratuberculosis* antigens, revealing the existence of a large number of previously unrecognized candidate diagnostic antigens. Enzyme-linked immunosorbent assay (ELISA) testing of 20 *M. avium* subsp. *paratuberculosis* recombinant proteins, representing reactive and nonreactive *M. tuberculosis* orthologs, further confirmed that the *M. tuberculosis* array has utility as a screening tool for identifying candidate antigens for Johne's disease diagnostics. Additional ELISA testing of field serum samples collected from dairy herds around the United States revealed that MAP2942c had the strongest seroreactivity with Johne's disease-positive samples. Collectively, our studies have considerably expanded the number of candidate *M. avium* subsp. *paratuberculosis* proteins with potential utility in the next generation of rationally designed Johne's disease diagnostic assays.

KEYWORDS antigens, *Mycobacterium*, protein array

Address correspondence to John P. Bannantine, john.bannantine@ars.usda.gov, or Vivek Kapur, vkapur@psu.edu.

Johne's disease is a chronic intestinal disease caused by infections in animals that are exposed to *Mycobacterium avium* subspecies *paratuberculosis* early in life (1). Despite the significant economic losses associated with Johne's disease in dairy cattle and sheep, progress in controlling infection has been significantly impeded by the lack of reliable and easy to use tests for detecting early infection. Over time, this results in infected animals shedding *M. avium* subsp. *paratuberculosis* into the environment and transmitting disease while appearing healthy. Extant enzyme immunoassays apply cumbersome and antiquated approaches to preparing immunodiagnostic antigens that

comprise whole-cell *M. avium* subsp. *paratuberculosis* extracts. Thus, by diluting sensitive and specific antigens buried within these complex extracts, the resulting assays have low levels of sensitivity for the detection of animals at early stages of infection. To address this shortcoming, we have initiated a program of protein antigen discovery based on the complete genome sequence of *M. avium* subsp. *paratuberculosis*.

The search continues for ideal antigens that can be used in antibody-based serological tests to control many infectious diseases. Animal producers want a test that predicts infection accurately and early, while private industry will only develop cheap, marketable tests. The latter eliminates DNA-based tests, and thus, researchers have focused on antibody-based tests because of lower cost. The use of purified recombinant proteins as antigens that specifically detect *M. avium* subsp. *paratuberculosis* will be among the critical diagnostic tools in Johne's disease detection, especially in the early, subclinical stages of disease. Our group has previously used protein arrays to screen for seroreactive antigens during early (subclinical) and late (clinical) stages of Johne's disease (2). Animals appear healthy in the subclinical stage, but they shed small numbers of bacteria in their feces intermittently, thus serving as a transmission source for herd mates. Animals in the clinical stage show disease signs, including weight loss, diarrhea, and consistent fecal shedding of bacteria. However, it can take several years for clinical signs to appear, making transmission difficult to stop in herds.

The *M. avium* subsp. *paratuberculosis* protein microarray is a tool that allows simultaneous determination of antibody responses to each spotted protein using only a small amount of serum and provides a fast, efficient approach to identify the most immunodominant proteins for low-cost diagnosis of Johne's disease. Furthermore, the immunodominant proteins identified by this approach may then be used to develop *M. avium* subsp. *paratuberculosis* peptide-based enzyme-linked immunosorbent assays (ELISAs) that identify infected animals in both clinical and subclinical stages of disease with high sensitivity and specificity. *M. avium* subsp. *paratuberculosis* protein arrays were previously constructed from a collection of greater than 600 expressed and purified *M. avium* subsp. *paratuberculosis* recombinant proteins (3). Early antigens were identified using an experimental infection model to track the developing humoral immune response in calves. Three antigens were identified for which antibodies were detected in calves by 70 days postinfection (4). Antigens during the later stages of Johne's disease were also identified in naturally infected cattle (2). However, these antigens are only the best of the subproteome represented on the protein array. The question that remains is, are they the best in the entire proteome?

Even if all of the recombinant *M. avium* subsp. *paratuberculosis* proteins that are currently available were spotted and analyzed on protein arrays, they would still comprise less than 20% of the predicted *M. avium* subsp. *paratuberculosis* proteome ($n = 4,350$), demonstrating that a large fraction of potential antigen candidates have yet to be screened. Given the time and costs associated with cloning, expressing, and purifying additional proteins from *M. avium* subsp. *paratuberculosis*, we explored the possibility of leveraging the availability of the whole-proteome microarray from *Mycobacterium tuberculosis* to screen for antigens useful in Johne's disease diagnostics. *M. tuberculosis* is the causative agent of human tuberculosis (TB) and is a related pathogen belonging to the same genus as *M. avium* subsp. *paratuberculosis*. The *M. tuberculosis* protein array has over 4,000 proteins spotted, which covers 99% of the *M. tuberculosis* proteome (5). This novel approach is the most ambitious unbiased screen of antigens ever undertaken for Johne's disease.

An *M. tuberculosis* proteome array was constructed and used previously to determine changes in the humoral immune response in patients with TB (5). Moreover, the array has been successfully applied to biomarker identification of active *M. tuberculosis* infection in a global collection of human serum and plasma samples (5). The principal finding was the identification of the immunoproteome, a set of antigens comprising 10% of the *M. tuberculosis* proteome that was highly reactive in *M. tuberculosis*-exposed individuals. Systems immunology analysis yielded a smaller subset of antigens associated with active *M. tuberculosis* infections with primarily extracellular secretory func-
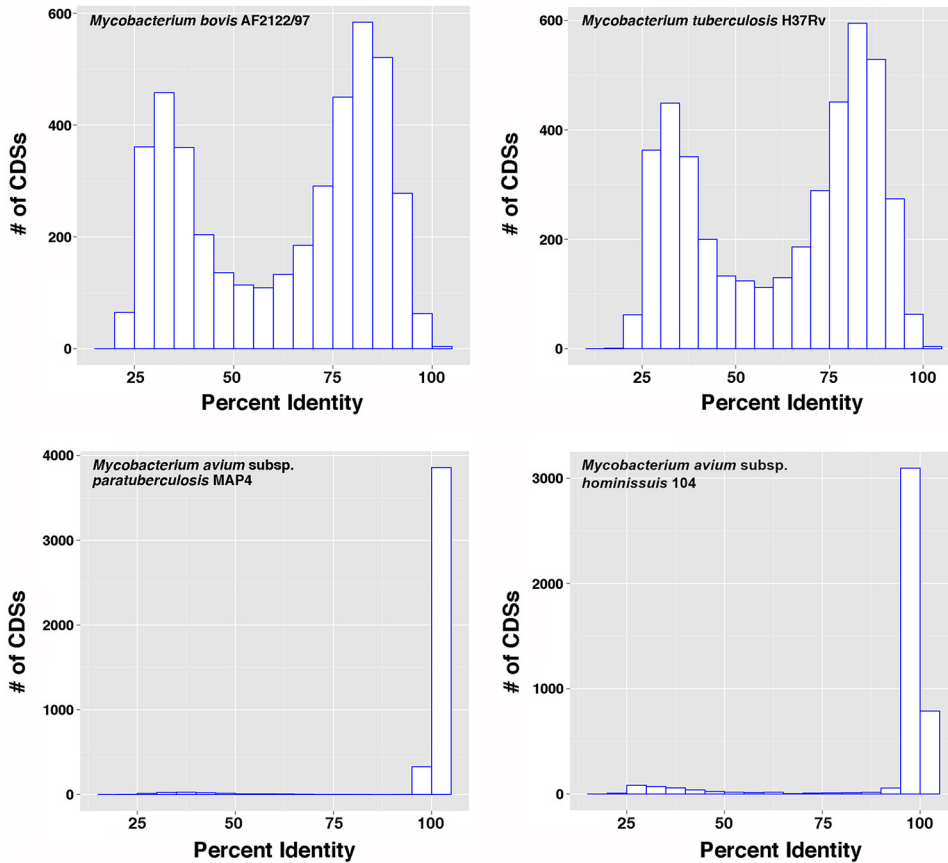
FIG 1 Distribution of pairwise comparisons of *M. avium* subsp. *paratuberculosis* strain K-10 with the mycobacterial species indicated on each graph. The histogram bars represent the frequency of CDS orthologs at a given percent identity.

tions. Diagnostic targets were further downselected after integrated analysis of humans and experimentally infected cynomolgus macaques (5). Collectively, these data led us to examine the utility of the *M. tuberculosis* protein array for Johne's disease antibody screening.

RESULTS

**Genome comparison of *M. avium* complex and *M. tuberculosis* complex strains.** The *M. avium* complex (MAC) consists of eight species, including *M. avium* (6). Within the *M. avium* species are four subspecies, *M. avium* subsp. *hominissuis*, *M. avium* subsp. *avium*, *M. avium* subsp. *silvaticum*, and *M. avium* subsp. *paratuberculosis*. All four subspecies are virtually identical at the genomic level (7, 8). Likewise, species within the *M. tuberculosis* complex are all highly similar based on genomic and proteomic comparisons (9). However, these two mycobacterial complexes are more distantly related to each other and are easily distinguishable. Thus, before investing in a strategy to leverage the *M. tuberculosis* protein array for Johne's disease studies, a genome scale comparative pairwise analysis of amino acid identities between orthologous MAC and *M. tuberculosis* complex proteins was performed. Analysis of *Mycobacterium bovis* and *M. tuberculosis* species from the *M. tuberculosis* complex showed a biphasic histogram with an average of 62% identity (range, 19% to 100%) among the protein-encoding genes with *M. avium* subsp. *paratuberculosis* strain K-10, and more than half of the orthologous proteins shared greater than 75% identity (Fig. 1), whereas the majority of coding DNA sequences (CDSs) from the MAP4 strain were at 100% identity and *M. avium* subsp. *hominissuis* strain 104 was at 95% percent identity or greater (Fig. 1). A complete list of percentages of identity of CDSs for sequenced mycobacterial
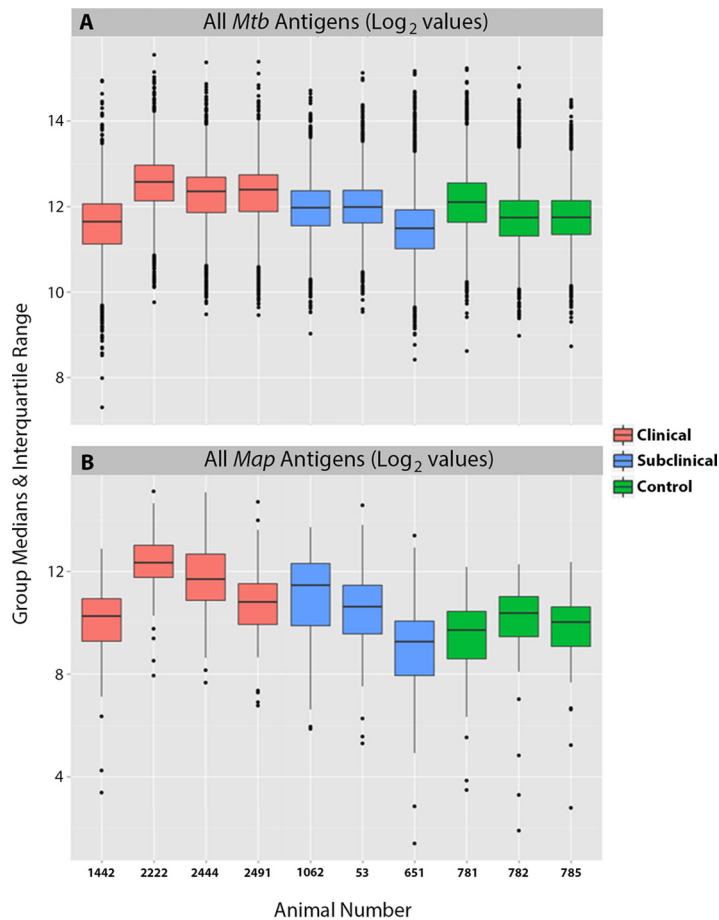
FIG 2 Box plots showing the overall distribution of antibody responses to *M. tuberculosis* and *M. avium* subsp. *paratuberculosis* proteins. Log$_2$-transformed signal intensities for each animal are shown in the box plots for *M. tuberculosis* proteins (A) and *M. avium* subsp. *paratuberculosis* proteins (B). The black horizontal bars, boxes, whiskers, and dots indicate the medians, ranges, 1.5 times the interquartile ranges, and outliers, respectively. The boxes are colored based on the health status of the animals.

genomes, using the MAP4 genome (10) as a reference, is presented in Table S1 in the supplemental material. Further bioinformatics analyses confirmed that the *M. tuberculosis* protein array contained more than 800 orthologs of *M. avium* subsp. *paratuberculosis* proteins that have been previously expressed (3). An additional 1,898 *M. tuberculosis* proteins with >60% identity to *M. avium* subsp. *paratuberculosis* orthologs are present on the *M. tuberculosis* array but are not among the *M. avium* subsp. *paratuberculosis* proteins that have been previously analyzed on a protein array (2, 4). Collectively, these data strengthened the hypothesis that the *M. tuberculosis* protein array might serve as a useful tool for screening over 1,800 additional candidate antigens for Johne's disease detection.

Protein array analysis of Johne's disease serum samples. To directly test the applicability of the *M. tuberculosis* array, 9 serum samples from cows with Johne's disease (6 clinical and 3 subclinical) and 3 serum samples from healthy control cows were probed using the *M. tuberculosis* whole-proteome array. For comparison, an *M. avium* subsp. *paratuberculosis* subproteomic array was also exposed to a subset of these serum samples. The log$_2$-transformed signal intensities of both the *M. tuberculosis* and *M. avium* subsp. *paratuberculosis* arrays are shown as box and whisker plots in Fig. 2. The raw and normalized signal intensities of the *M. tuberculosis* protein array are shown in Fig. S1 in the supplemental material. The results revealed a total of 729 *M. tuberculosis* antigens that were reactive to at least one of the serum samples from cows with Johne's disease and had a mean intensity greater than 10 (see Table S2 in the
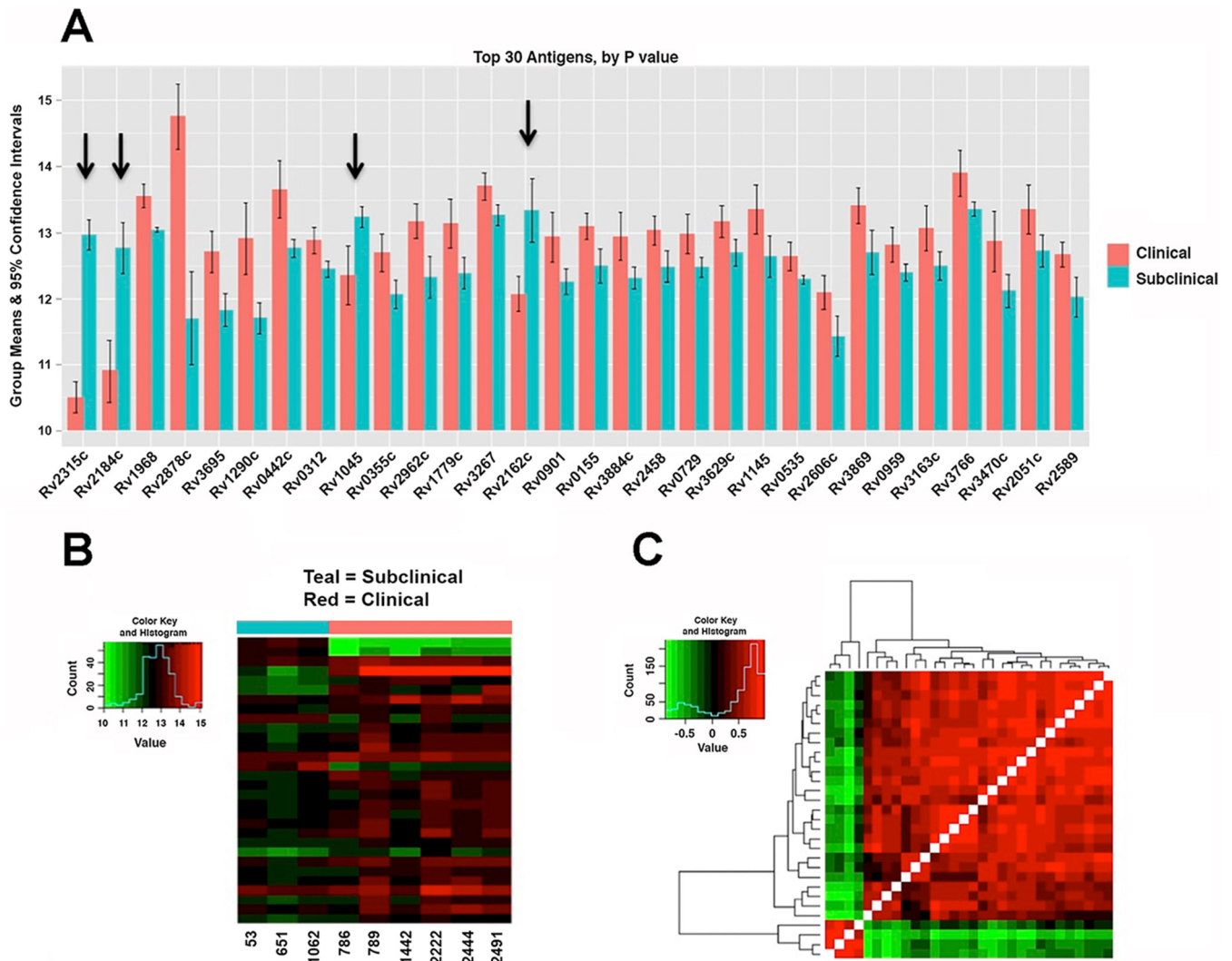
FIG 3 *M. tuberculosis* proteins showing differential antibody reactivity by disease state. (A) Differences among the top 30 antigens between cows in the clinical and subclinical stages of disease ordered from left (lowest *P* value) to right (highest *P* value, based on Student's *t* test). See Table S3 in the supplemental material for confidence intervals, *P* values, and adjusted *P* values. The bars represent the means of log₂-transformed data, and the error bars represent 95% confidence intervals. The arrows mark candidate antigens that are higher in animals in the subclinical stage of disease. (B) Heat map of the log₂-transformed signals for the top 30 antigens ordered by subclinical and clinical groups. Serum sample numbers are along the bottom, and genes are stacked in the same order as in panel A. (C) Hierarchical clustering of the correlations between antigen reactivities. Red shows highly correlated responses, and green is uncorrelated responses, which may highlight diagnostic markers.

supplemental material), 552 of which had an *M. avium* subsp. *paratuberculosis* ortholog with identity above 70%, suggesting that this approach has identified hundreds of new seroreactive *M. avium* subsp. *paratuberculosis* orthologs as potential antigen candidates for future analysis. The top 30 *M. tuberculosis* proteins showing differential antibody responses between cows in clinical and subclinical stages of disease are shown in Fig. 3A with additional information about each protein listed in Table S3 in the supplemental material. While most antigens had stronger antibody responses in cows in the clinical stage of disease, four of the proteins showed significantly greater reactivity with antibodies from animals in the subclinical stage of disease, suggesting potential early detection antigens (Fig. 3A). Three of these proteins are annotated as hypothetical proteins (Rv1045, Rv2184c, and Rv2315c), while Rv2162c is a PE-PGRS family protein (11). Collectively, antibody reactivity is stronger for animals in the clinical stage of disease than for animals in the subclinical stage of disease (Fig. 3B), and correlation of antibody responses is strong overall, but the four proteins mentioned above (Rv1045, Rv2315c, Rv2184c, and Rv2162c) lacked correlated responses, which may be indicative of unique diagnostic markers (Fig. 3C).

TABLE 1 *M. avium* subsp. *paratuberculosis* proteins with the highest infection-to-control ratios

MAP ID	Mtb ID	% Identity	SubClinical/Neg[a]	Clinical/Neg[b]	Cy5[c]	Description	Reference
MAP0067	Rv0053	95.83%	3.54	1.91	17795	30S ribosomal protein S6 rpsF	Not published
MAP0186c	Rv3847	96.61%	3.72	2.44	23151	Hypothetical protein	Not published
MAP0654	Rv0820	89.92%	1.62	10.81	1142	Probable phosphate-transport ATP-binding protein	Not published
MAP0847	Rv1754c	61.48%	1.54	6.95	2172	hypothetical protein	Not published
MAP0856c	Rv2590	29.17%	2.22	6.4	1746	Probable fatty-acid-CoA ligase FadD9	Not published
MAP1012c	Rv1063c	76.29%	2.8	3.5	20784	hypothetical protein	41
MAP1272c	Rv1566c	77.21%	1.16	7.09	1636	invasion-associated protein	17, 22, 42
MAP1346c	Rv1354c	56.40%	3.11	4.57	14094	conserved hypothetical protein	Not published
MAP1781	Rv2046	61.06%	1.81	7.85	1582	lipoprotein lppl	Not published
MAP2121c	NA[d]		2.49	14.39	20102	invasion-associated protein	17, 20, 21
MAP2677c	Rv0546c	26.27%	2.8	3.61	14005	conserved hypothetical protein	2, 43
MAP2942c	Rv2878c	72.51%	0.62	6.19	2397	soluble secreted antigen mpt53 precursor	16, 43
MAP3184	Rv3136	49.63%	3.66	1.8	17507	hypothetical protein (related to PPE family)	16
MAP3195	Rv0273c	31.03%	1.34	4.85	3905	transcriptional regulator	Not published
MAP3217c	Rv3163c	93.62%	2.99	3.01	17303	conserved secreted protein	Not published
MAP3422c	Rv3300c	77.86%	3.07	4.62	17652	conserved hypothetical protein	Not published
MAP3776c	Rv2059	35.27%	1.85	5.19	1799	closely related to periplasmic solute binding proteins	Not published
MAP3812c	Rv1433	74.91%	1.52	7.26	1008	hypothetical exported protein	Not published
MAP3890	Rv0450c	59.77%	3.93	1.71	25861	transmembrane transport protein mmpL4	Not published
MAP4264	Rv3418c	97.00%	3.25	1.84	30012	10 kda chaperonin groES	Not published

[a]Ratio of average intensities of sera from cows in the subclinical stage of disease to the average intensity of sera from negative cows. Green highlighting shows antigens with stronger subclinical antibody responses than clinical antibody responses.
[b]Ratio of average intensities of sera from cows in the clinical stage of disease to the average intensity of sera from negative cows. Yellow highlighting shows antigens with stronger clinical antibody responses than subclinical antibody responses.
[c]Cy5–anti-MBP used to determine spot intensities/local correction of signal.
[d]NA, no ortholog in *M. tuberculosis* (Mtb).

Several *M. tuberculosis* proteins that showed the strongest antibody reactivity with Johne's disease serum were also orthologous to known *M. avium* subsp. *paratuberculosis* antigens. For example, the strongest antibody response among cows with clinical Johne's disease was that of Rv1860, a proline-rich secreted protein showing a mean signal intensity of 15.3 (see Table S2 in the supplemental material). The *M. avium* subsp. *paratuberculosis* ortholog of this protein is MAP1569, which has been observed as a strong antigen in multiple serological screening approaches (12–15). The second strongest antigen among the cows in the clinical stage of disease was Rv2878c, which is homologous to MAP2942c, another known antigen in *M. avium* subsp. *paratuberculosis* (16). Other published *M. avium* subsp. *paratuberculosis* antigens identified as orthologs in Table S2 are MAP0210c (16), MAP0900 (2), and MAP2121c (17). However, *M. avium* subsp. *paratuberculosis* orthologs for most of the *M. tuberculosis* antigens identified in this study have not been described in the literature, suggesting they are new candidate diagnostic antigens for Johne's disease. Finally, 6 of the top 10 proteins identified from the clinical disease stage were also ranked among the top 10 in the subclinical disease stage (see Table S2), suggesting that these antigens may be detected throughout the progression of this chronic disease.

The top 20 proteins with the highest infected-to-negative ratios on the *M. avium* subsp. *paratuberculosis* partial protein array are shown in Table 1. A 6.40 clinical-to-negative ratio was observed for MAP0856c, the gene for which is present on a genomic island unique to *M. avium* subsp. *paratuberculosis* (18, 19), making it a particularly interesting diagnostic candidate. The strongest ratio overall is 14.39 from MAP2121c, a membrane protein that has been suggested as an antigen in the past (17, 20, 21) and whose ortholog (Rv3347c) was ranked 33rd on the *M. tuberculosis* array (see Table S2 in the supplemental material). Other known *M. avium* subsp. *paratuberculosis* antigens that appear among the top 10 clinical-to-negative ratios in Table 1 are MAP2942c (16) and MAP1272c (22). The top 20 *M. tuberculosis* proteins with the highest ratios are listed in Table S4 in the supplemental material.
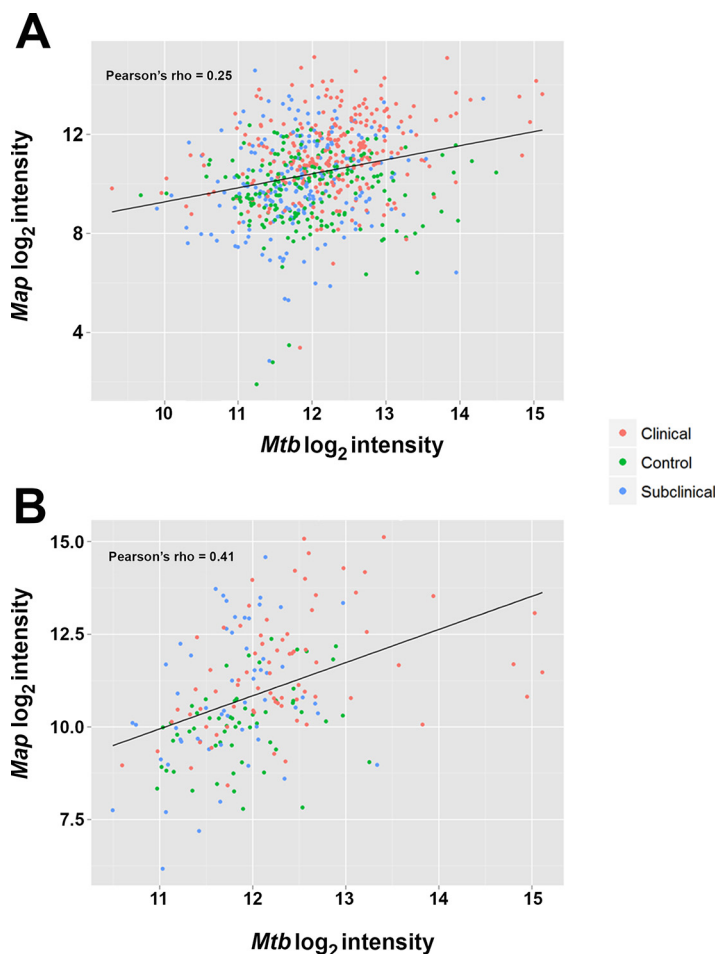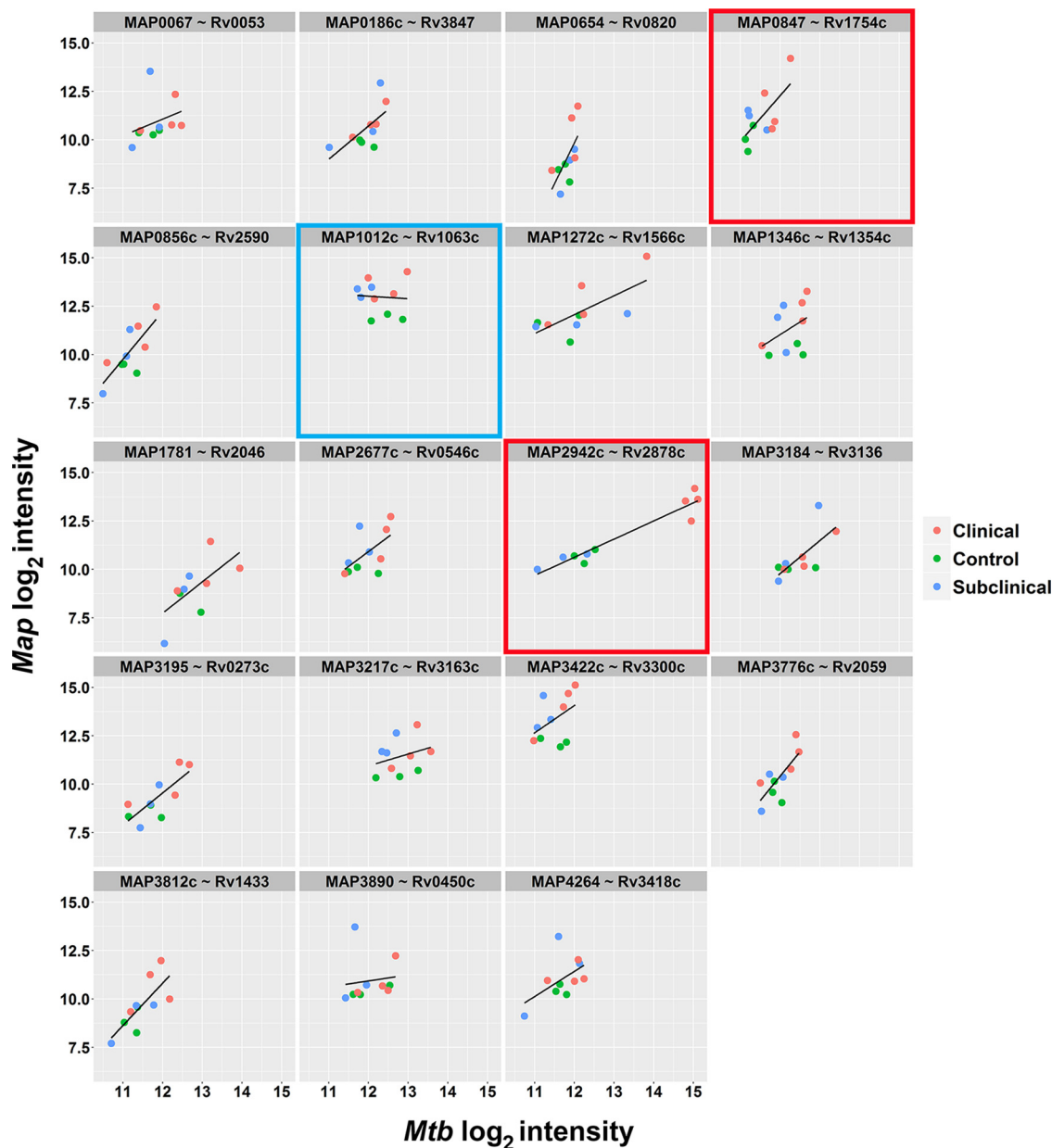
FIG 4 Correlation between *M. avium* subsp. *paratuberculosis* (Map) and *M. tuberculosis* (Mtb) proteins. (A) All orthologous genes. (B) The top antigens. Pearson's correlation is indicated in each plot.

Correlation of *M. avium* subsp. *paratuberculosis* and *M. tuberculosis* proteins. Correlation between the seroreactivity of antigens on the *M. avium* subsp. *paratuberculosis* protein array and orthologs on the *M. tuberculosis* array was next examined. By taking the log$_2$-transformed data, Pearson's rho was 0.25 among all unique matches, suggesting poor correlation (Fig. 4A). However, correlation among the top antigens identified on the *M. avium* subsp. *paratuberculosis* and *M. tuberculosis* arrays was stronger, with a value of 0.41 and good clustering even among proteins that had relatively low levels of identity (Fig. 4B). Although preliminary, these data suggest that *M. tuberculosis* orthologs on the *M. tuberculosis* arrays react to sera from *M. avium* subsp. *paratuberculosis*-infected cows in a manner similar to what is observed with the purified proteins spotted on the *M. avium* subsp. *paratuberculosis* array.

The distribution of reactivity for the top *M. avium* subsp. *paratuberculosis* antigens listed in Table 1, along with the corresponding *M. tuberculosis* proteins, was examined at the antigen level, along with how they correlated among disease statuses (Fig. 5). Representative subplots are highlighted and show antigens that display good seroreactive correlation with both *M. avium* subsp. *paratuberculosis* and *M. tuberculosis* proteins (Fig. 5, red boxes), as well as examples where the *M. avium* subsp. *paratuberculosis* antigen was a better predictor for clinical disease (Fig. 5; blue box). Those that displayed good correlation also had high amino acid identity. For example, the *M. avium* subsp. *paratuberculosis* protein MAP4264 was 97% identical to Rv3418c in *M. tuberculosis* (Fig. 5).

Next, the distribution of reactivity for the antigens listed in Table 1 at the individual animal level from the *M. avium* subsp. *paratuberculosis* array and their correlation with

FIG 5 Correlation of seroreactive *M. avium* subsp. *paratuberculosis* antigens with *M. tuberculosis* proteins. The lattice plots show log$_2$-transformed data for *M. avium* subsp. *paratuberculosis* antibody responses (*y* axis) versus *M. tuberculosis* antibody responses (*x* axis). Each subplot represents one of the top reactive *M. avium* subsp. *paratuberculosis* antigens (from Table 1) with the corresponding orthologous *M. tuberculosis* antigen. Individual subjects are plotted for each antigen combination and color coded by clinical group. A line of best fit is drawn for each subplot. The plots boxed in red indicate good seroreactive correlation with both *M. avium* subsp. *paratuberculosis* and *M. tuberculosis* proteins. The plot boxed in blue indicates where *M. avium* subsp. *paratuberculosis* antigen was the best predictor of Johne's disease. MAP2121c is missing because there is no *M. tuberculosis* ortholog for the gene.

the *M. tuberculosis* array were examined (Fig. 6). The results show, on average, good correlation between the two arrays for each individual animal, as indicated by positive slopes. However, two animals (53 and 2444) showed poor correlation, with slopes near zero (Fig. 6). Collectively, these results suggest that the *M. tuberculosis* arrays will provide a mechanism for the triage of *M. avium* subsp. *paratuberculosis* orthologs, especially those with high identity but that are not seroreactive with sera from infected animals or those that appear to be equally reactive with negative sera and infected cows, representing targets that can be excluded from the list that may be predictive from an *M. avium* subsp. *paratuberculosis* diagnostic assay development standpoint.
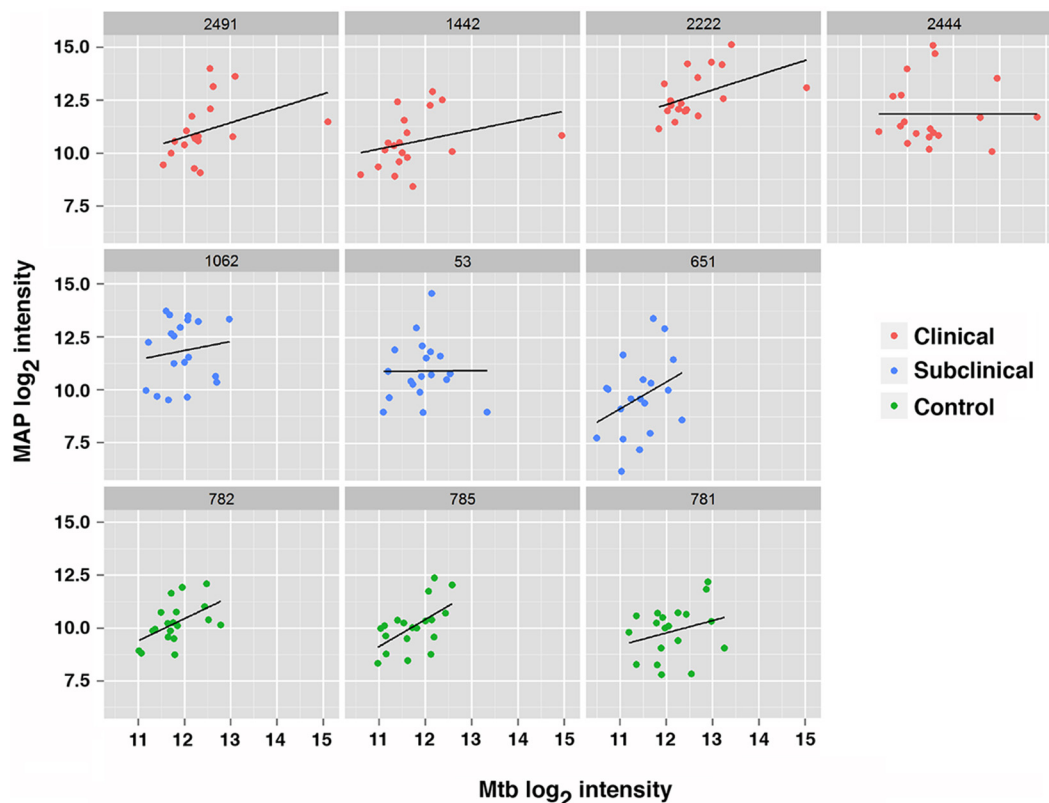
**FIG 6** Correlation of the top seroreactive *M. avium* subsp. *paratuberculosis* antigens with *M. tuberculosis* proteins analyzed by individual cow. The lattice plots show $\log_2$-transformed data for *M. avium* subsp. *paratuberculosis* antibody responses (*y* axis) against antibody responses to *M. tuberculosis* proteins (*x* axis). Each subplot represents the responses from one study cow, and the dots represent the top reactive *M. avium* subsp. *paratuberculosis* antigens with the corresponding orthologous *M. tuberculosis* antigens. Individual subjects are plotted for each antigen combination and color coded by clinical group. A line of best fit is drawn for each subplot. MAP2121c was not included because there is no *M. tuberculosis* ortholog for the gene.

Reactivity of *M. avium* subsp. *paratuberculosis* orthologs by ELISA. To test the ability of the *M. tuberculosis* protein array to discriminate and rank strong antigens for Johne's disease antibody tests, 10 *M. avium* subsp. *paratuberculosis* recombinant protein orthologs corresponding to *M. tuberculosis* reactive proteins (see Table S2 in the supplemental material) were selected, along with 10 recombinant protein orthologs corresponding to low-reactive or nonreactive *M. tuberculosis* proteins (not listed in Table S2). ELISAs with the same serum samples from the protein array study were used to evaluate these 20 *M. avium* subsp. *paratuberculosis* proteins. MAP2942c was clearly the strongest antigen among the proteins, with an average optical density (OD) reading of 1.3 (Fig. 7A). This was also the only recombinant protein that demonstrated higher reactivity than the whole-cell extract (Fig. 7A, K-10 sonicate). The *M. tuberculosis* ortholog for the protein is Rv2878c, which ranked second among all the antigens tested with sera from cows with clinical disease (Table S2).

The same 20 recombinant proteins were further tested using a set of well-characterized serum samples from dairy cows around the United States. The MAP2942c protein was once again the strongest antigen in this serum set. Comparing *M. avium* subsp. *paratuberculosis* orthologs of the *M. tuberculosis* reactive and nonreactive proteins showed significance (analysis of variance [ANOVA]; $P < 0.05$) for both the positive and negative serum repository samples (Fig. 7B). The mean sample-to-positive (S/P) ratios were significantly higher ($P < 0.05$) among the reactive *M. avium* subsp. *paratuberculosis* orthologs in the clinical and positive serum groups as measured by ELISA (Fig. 8). Collectively, these data demonstrate that *M. avium* subsp. *paratuberculosis* orthologs of the antigenic *M. tuberculosis* proteins are able to distinguish *M. avium* subsp. *paratuberculosis*-infected cows from healthy cows.
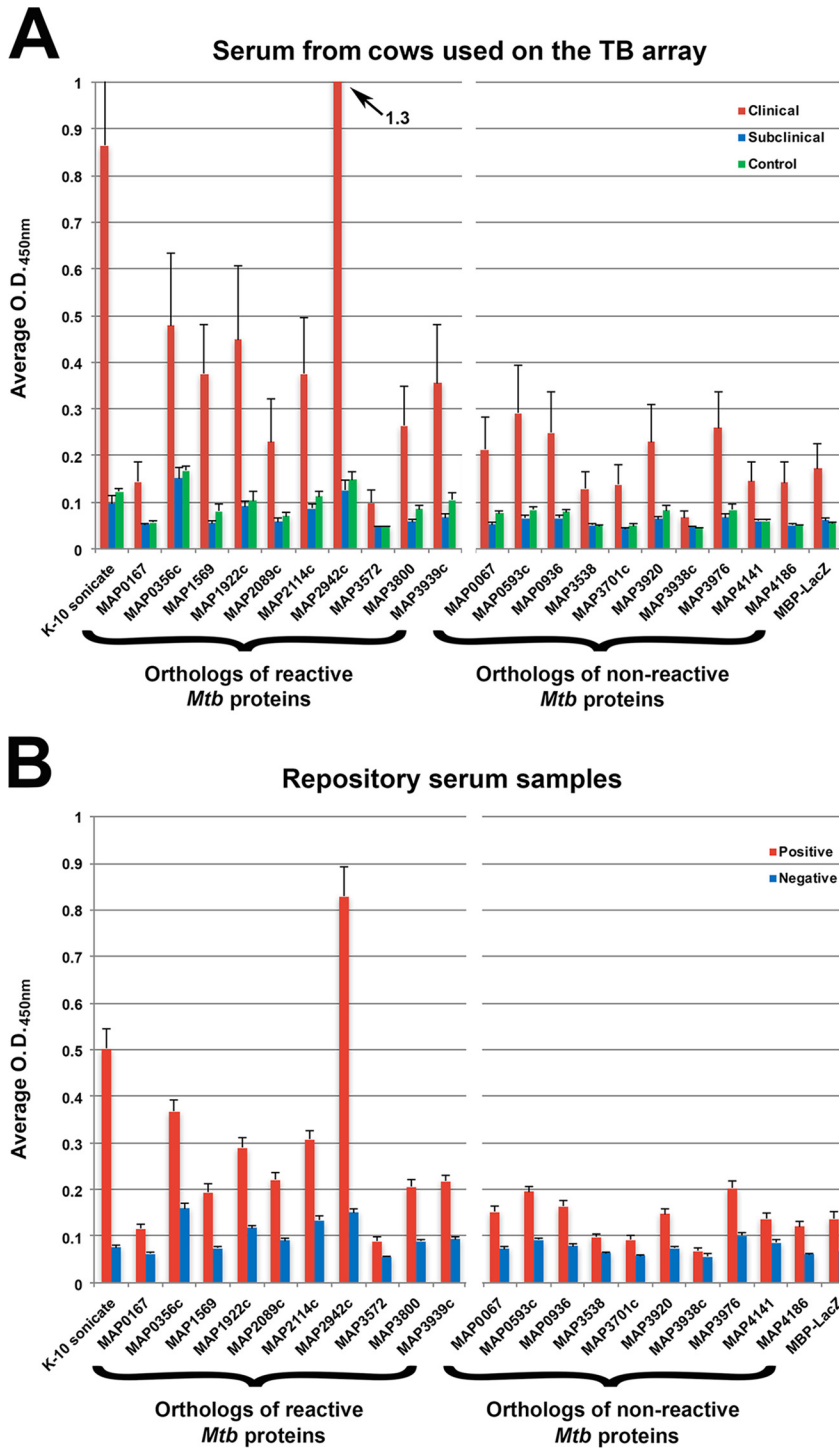
FIG 7 The humoral immune response against *M. avium* subsp. *paratuberculosis* recombinant proteins confirms strong antigens identified from the *M. tuberculosis* array. Serum immunoglobin levels from healthy and Johne's disease cattle were analyzed by ELISA. Shown are the mean optical density values for each protein against labeled serum samples. The *M. avium* subsp. *paratuberculosis* orthologs to reactive *M. tuberculosis* proteins (from Table S2 in the supplemental material) are grouped on the left, and orthologs to nonreactive *M. tuberculosis* proteins (not listed in Table S2) are grouped on the right. The error bars represent the standard errors of the mean (SEM). (A) ELISA analysis was performed using the same serum set as in the *M. tuberculosis* array study (Table 2). (B) An expanded serum set from well-characterized dairy herds around the United States was used to further test the same recombinant protein set (see Table S5 in the supplemental material). A total of 30 negative and 42 positive serum samples were analyzed. The results are shown as means and SEM and were compared using analysis of variance (ANOVA) for the 10 reactive versus 10 nonreactive *M. avium* subsp. *paratuberculosis* orthologs for the positive and negative repository serum samples.
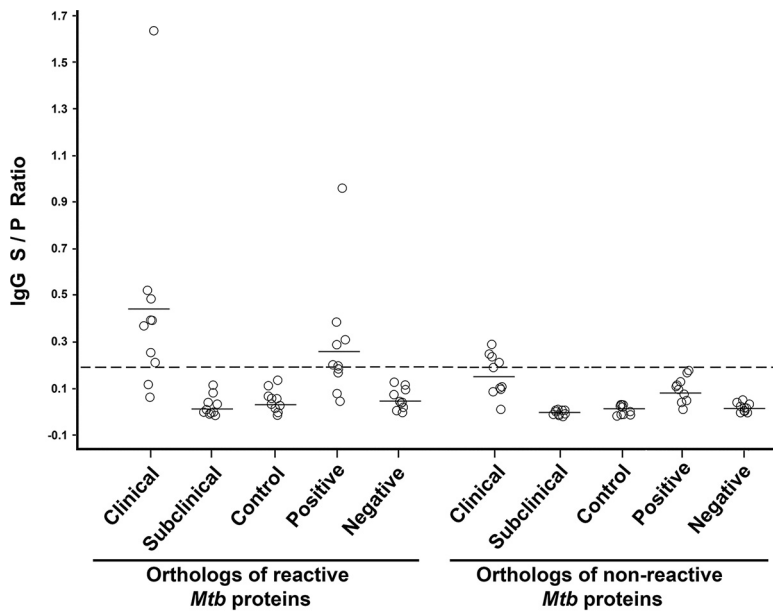
FIG 8 Distribution of reactive and nonreactive *M. avium* subsp. *paratuberculosis* othologous proteins with Johne's disease-positive and -negative serum samples. The results are expressed as the sample-to-positive ratio, where ≥0.2 was considered positive. The circles represent *M. avium* subsp. *paratuberculosis* recombinant proteins. The horizontal bars represent the means. The cutoff value of 0.2 is indicated by the dashed horizontal line.

DISCUSSION

Although *M. avium* subsp. *paratuberculosis* and *M. tuberculosis* are related mycobacterial species, belonging to their own complexes within the genus, the results of our investigations suggest there is sufficient antigenic cross-reactivity to leverage the *M. tuberculosis* array for Johne's disease studies. By using the *M. tuberculosis* protein array to test sera from cows with Johne's disease, known *M. avium* subsp. *paratuberculosis* antigens were confirmed and hundreds of new potential antigens were identified. This study may represent the largest, unbiased screen of antigens ever undertaken for Johne's disease. Furthermore, the screen, combined with a large collection of recombinant proteins, makes it possible to construct a diagnostic platform that could range from ELISA to miniature lateral-flow-based tests.

The results of this study have the side benefit of documenting a majority of the *M. bovis* proteins that cross-react with *M. avium* subsp. *paratuberculosis*, since *M. bovis* is so closely related to *M. tuberculosis*. This is important, because *M. bovis* is also a pathogen of cattle that has important regulatory consequences (23–25), and vaccination efforts against either pathogen ideally should not interfere with diagnostic tests for the other (26, 27). The data obtained in this study make it possible to systematically determine cross-reactive antigens, as well as antigens that may distinguish each pathogen. Armed with this new information, vaccine and diagnostic strategies for either disease are better informed.

An important component of this study is the assembly of well-characterized serum samples to enable identification of potent antigens for early and late diagnosis of Johne's disease. Sera were obtained from cows, along with longitudinal clinical information so that they could be stratified by the various stages of Johne's disease. Although the repository serum samples could not be included in the *M. tuberculosis* array study due to costs associated with printing and processing, these additional, well-characterized sera enabled further refinement of the best antigens in the ELISA study.

Through this approach, antigens were identified in both clinical and subclinical groups in comparison with the ratio of intensities to those of the negative-control

group. As expected, different patterns of serum antibody responses were observed for cattle in clinical and subclinical stages of disease, with overall stronger responses noted for cows in the clinical stage of disease. These results corroborate the paradigm of a progressive increase in antibody response to *M. avium* subsp. *paratuberculosis* infection as animals transition to more advanced stages of disease (28). Among the top 30 *M. tuberculosis* antigens, ranked by *P* value, only 4 showed stronger antibody reactivity in cows in the subclinical stage of disease. Notably, three of these antigens are annotated as hypothetical proteins, suggesting that proteins that are antigenic in the subclinical stage not only are rare but also not well characterized.

From observed differences between the two disease stages, a dynamic antibody response to some proteins detected during subclinical Johne's disease disappears during the clinical stage, and the immunodominant antigens recognized by clinical sera may not be recognized by subclinical-stage antibody responses. The hypothesis still needs to be tested on an expanded set of samples from large-scale serum collections that have recently been established for Johne's disease studies. Data obtained from the current study indicated these expanded studies are feasible and hence will be undertaken.

According to one study describing antibody responses to the *M. tuberculosis* proteome, 484 out of 4,099 *M. tuberculosis* proteins were recognized as antigenic by sera from 240 TB patients (5), and we estimate that the *M. avium* subsp. *paratuberculosis* proteome will have a similar number when tested with sera from Johne's disease cattle. Using these 484 *M. tuberculosis* proteins, we searched the *M. avium* subsp. *paratuberculosis* genome and found 361 orthologs, accounting for 74.6% of the potential *M. avium* subsp. *paratuberculosis* antigens identified in the *M. tuberculosis* study. About 70% of these orthologs are not present on the *M. avium* subsp. *paratuberculosis* array but will be included in a second-generation *M. avium* subsp. *paratuberculosis* protein array. Bioinformatics analysis could then be used to compare epitopes and further narrow the number of *M. avium* subsp. *paratuberculosis* proteins missing from a whole-immunoproteome analysis.

We hypothesized that the most immunodominant proteins would be identified by comparison between infected cattle and negative controls, as was done previously using the *M. tuberculosis* microarray, where 13 proteins were identified as associated with active TB (5). A major challenge with the current technology is to accurately classify *M. avium* subsp. *paratuberculosis*-infected animals in different disease statuses, particularly true-negative animals. However, another group has developed a Bayesian methodology (29, 30) that allows us to estimate the sensitivity and specificity of a new test even if we do not know the gold standard. This technique has been applied to the development of a multiplex assay for the detection of antibodies to *Borrelia burgdorferi* in horses (31), and it will be employed in future studies with a larger set of Johne's disease cows.

Antibody screening with *M. tuberculosis* microarrays has identified new antigenic proteins that are not in our collection of *M. avium* subsp. *paratuberculosis* recombinant proteins. However, we realize that the proteins identified with an *M. tuberculosis* microarray may not all be good candidates because the high identity of amino acid sequences may contribute to cross-reactivity. Likewise, nonreactive proteins on the *M. tuberculosis* microarray may not be indicative of nonreactivity in *M. avium* subsp. *paratuberculosis* orthologs. Whereas negative responses may represent true negatives in corresponding *M. avium* subsp. *paratuberculosis* orthologs (which will be a majority of cases), sera may not recognize *M. tuberculosis* proteins, not because the corresponding orthologs in *M. avium* subsp. *paratuberculosis* are not immunodominant, but because the two orthologs are too different at the amino acid level.

Despite this, proteins showing the highest intensity were readily identified. The most prominent protein from the ELISA study was MAP2942c, termed a Mpt53 secreted antigen, which has been annotated as a disulfide oxidoreductase and was previously identified by screening an expression library with sera from a cow in the clinical stage of disease (16). In addition, the gene encoding this protein showed increased tran-

scription in the presence of iron (32) and the rhodamine agent D157070 (33). MAP2942c had the second highest intensity in clinical disease but was among the weakest reactors in animals in the subclinical stage of disease, based on the *M. tuberculosis* array. Likewise, MAP1569, another secreted antigen, was strongest during clinical disease but 145th during subclinical disease (see Table S2 in the supplemental material). The protein has been shown to activate dendritic cells and stimulate gamma interferon (IFN-γ) production (34). Membrane proteins, fatty acid-coenzyme A (CoA) synthase, and cytochrome *c* oxidase are among the strongest reactors during subclinical disease.

The analysis showed that 1,916 *M. tuberculosis* proteins had at least 75% amino acid identity to *M. avium* subsp. *paratuberculosis*; however, there are 1,805 *M. avium* subsp. *paratuberculosis* proteins with identities to *M. tuberculosis* proteins below 60%. Even though 327 of these low-identity proteins are already represented on an existing *M. avium* subsp. *paratuberculosis* array (unpublished data), the remainder represent proteins that are not likely amenable to analysis by using only the *M. tuberculosis* array. Nonetheless, the results suggest that the *M. tuberculosis* protein microarray can be successfully applied to *M. avium* subsp. *paratuberculosis* antibody screening, since it will add greatly to the number of testable candidate antigens. To overcome these limitations and until whole-proteome *M. avium* subsp. *paratuberculosis* arrays become available, future studies will need to consider applying sophisticated bioinformatics and statistical analysis tools to analyze the *M. avium* subsp. *paratuberculosis* orthologs of all positive and negative spots to make a meaningful determination on selection of *M. avium* subsp. *paratuberculosis* protein candidates to pursue in antigen-based diagnostic assays.

MATERIALS AND METHODS

Comparative genome analysis. The genome sequence of *M. avium* subsp. *paratuberculosis* strain K-10, a bovine isolate from a Wisconsin dairy herd, was compared to those of *M. avium* subspecies *hominissuis* strain 104, *M. bovis* AF2122/97, and *M. tuberculosis* H$_{37}$Rv. *M. avium* subsp. *paratuberculosis* strain MAP4, a human isolate (10), was also used in these analyses. The number of amino acid matches was determined by pairwise analysis for all CDSs in each genome and plotted as percent identity on a histogram.

***M. tuberculosis* and *M. avium* subsp. *paratuberculosis* protein array content and spotting.** Antigen Discovery, Inc. (ADI), Irvine, CA, has developed protein microarrays for antibody screening of *M. tuberculosis*, *Brucella*, and malaria infections (5, 35, 36), as well as other prominent diseases. Therefore, the *M. tuberculosis* array was fabricated by ADI as previously described (5, 37). Briefly, using *M. tuberculosis* H$_{37}$Rv genomic DNA as a template, all the open reading frames were amplified using custom PCR primers. Genes greater than 3 kb in length were amplified as multiple overlapping fragments. PCR products were cloned into a linearized T7 vector, pXI, using *in vivo* recombination cloning. Using individually purified plasmids, *M. tuberculosis* proteins were expressed in an *Escherichia coli*-based *in vitro* transcription and translation (IVTT) system (5 Prime, Gaithersburg, MD). The resulting IVTT reactions were printed as single spots without further purification on custom 3-pad nitrocellulose-coated Avid slides (Grace Bio-Labs, Bend, OR) using an OmniGrid Accent microarray printer (Digilabs, Inc., Marlborough, MA) in 4-by-4 subarray format, with each subarray comprising 18 by 18 spots. The total number of *M. tuberculosis* proteins spotted was 3,963, representing 3,864 genes (3,722 genes in the current NCBI gene set and 142 pseudogenes from prior gene sets). Among them, 48 genes of >3 kb were fragmented into a total of 133 segments. Each subarray included negative-control spots carrying IVTT reaction mixtures without DNA templates, purified protein spots of previously identified *M. tuberculosis* biomarkers, and positive-control spots for hybridization.

For the *M. avium* subsp. *paratuberculosis* array, 108 purified *M. avium* subsp. *paratuberculosis* K-10 recombinant proteins were selected (shown in red in Table S1 in the supplemental material) from a recombinant protein collection (3) based on the available quantity and identity to *M. tuberculosis* orthologs. In addition, 33 control spots were included for duplicate printing onto SuperEpoxy 2 glass slides (ArrayIt, Sunnyvale, CA) using an OmniGrid 100 microarray printer. The control spots included unconjugated bovine IgG (serially diluted) and mouse IgG for secondary-antibody binding. Additional controls included defined peptides, such as maltose binding protein (MBP) and cell extracts from *M. avium* subsp. *avium*, *M. avium* subsp. *hominissuis*, *Mycobacterium intracellulare*, *Mycobacterium smegmatis*, and *Mycobacterium scrofulaceum*. The negative controls included rabbit IgG, phosphate-buffered saline (PBS), and array-printing buffer. All *M. avium* subsp. *paratuberculosis* recombinant proteins were expressed as MBP fusions and affinity purified as described previously (38). Epoxy-activated slides were used, since they enable high-density printing and strong protein attachment via covalent cross-linking and high-resolution detection (39). Proteins were spotted at concentrations of 0.10 to 0.20 μg/μl. To determine maximum spot intensities and local background correction, *M. avium* subsp. *paratuberculosis* arrays were probed with monoclonal antibodies to the maltose binding protein tag. The amounts of

TABLE 2 Health status of cattle used in this study

| Cow identifier | Disease status | Test result | | Fecal PCR[c] | |
		IDEXX ELISA[a]	IFN-γ[b]	IS900	ISMap02
781	Control	0.073	0.063/0.077	Neg	Neg
782	Control	0.048	0.059/0.145	Neg	Neg
785	Control	0.058	0.113/0.148	Neg	Neg
53	Subclinical	0.046	0.120/0.474	Neg	27.95
651	Subclinical	0.023	0.124/0.279	Neg	Neg
1062	Subclinical	0.053	0.141/1.468	Neg	Neg
786	Clinical	2.94	0.044/0.084	26.28	16.62
789	Clinical	2.26	0.196/0.598	22.43	Neg
1442	Clinical	2.62	0.043/0.083	26.13	18.1
2222	Clinical	2.96	0.178/1.479	25.83	20.66
2444	Clinical	3.07	0.089/0.124	30.05	20.64
2491	Clinical	3.26	0.088/0.103	33.74	19.4

[a]A negative ELISA result is defined as less than 0.1.
[b]Values are reported as no stimulation/antigen stimulation. A negative IFN-γ test result is anything less than 0.11.
[c]A negative (Neg) fecal PCR result is a threshold cycle (C_T) value higher than 35. IS900 has 17 copies per genome, while ISMap02 has 6 copies per genome.

protein spotted varied slightly, and this was taken into account in our analysis. All protein array slides were stored for no more than 3 days in a desiccator cabinet at 4°C until they were ready for probing with bovine serum samples.

Bovine serum samples. Serum samples used on the *M. tuberculosis* protein arrays were from Holstein cows, including six in the clinical stage of disease and three in the subclinical stage, along with three healthy control cows (Table 2). The same set of serum samples, with the exception of 786 and 789, was also used on the *M. avium* subsp. *paratuberculosis* protein arrays. All of these cows were housed at the USDA National Animal Disease Center in Ames, IA, and have an approved IACUC protocol. Furthermore, all the cows with Johne's disease acquired the infection naturally. All the cows have documented health histories and are tested quarterly by ELISA, IFN-γ response, and fecal culture. Table 2 shows the results of these tests at the time the bleed was taken for this study. Control cows were defined as Johne's disease free by negative serum ELISA (IDEXX, Westbrook, ME), IFN-γ (Bovigam; ThermoFisher Scientific, Waltham, MA), and fecal PCR tests. Animals in the clinical stage of disease showed Johne's disease symptoms, which included shedding bacteria in the feces, and a positive serum ELISA result using an *M. avium* subsp. *paratuberculosis* antibody test kit (IDEXX). The subclinical stage of disease is not as clearly defined, but animals in this stage are typically IFN-γ positive and may be intermittently shedding low numbers of bacteria in their feces. All animals were skin test negative for bovine TB.

While the same serum samples were also used in the ELISA validation experiment, an additional 73 well-characterized bovine serum field samples from the Johne's Disease Integrated Program Repository were also included in this experiment (see Table S5 in the supplemental material). The repository samples were classified into two groups based on three commercial ELISAs, as well as fecal culture and fecal PCR (Table S5). The positive group consisted of 42 samples that were fecal culture positive and ELISA positive and the negative group consisted of 30 samples from negative low-exposure cows.

Probing protein microarrays. Prior to incubation with serum, the *M. tuberculosis* and *M. avium* subsp. *paratuberculosis* arrays were rehydrated and blocked for 30 min using protein array blocking buffer (10485356; Maine Manufacturing, Sanford, ME) at room temperature. Serum/plasma samples were diluted 1:200 in blocking buffer and incubated on arrays at 4°C overnight with gentle agitation. The arrays were washed 3 times in wash buffer (Tris-buffered saline [TBS] with 0.05% Tween 20). Bound IgG antibodies were detected with either a biotinylated anti-bovine secondary antibody (Jackson ImmunoResearch, West Grove, PA), followed by incubation with SureLight P-3 fluorochrome conjugated to streptavidin (Columbia Biosciences, Columbia, NY) for *M. tuberculosis* arrays or Cy3-conjugated anti-goat IgG (Jackson ImmunoResearch, West Grove, PA) for *M. avium* subsp. *paratuberculosis* arrays. The *M. avium* subsp. *paratuberculosis* array consisted of MBP-tagged recombinant proteins; thus, Cy5–anti-MBP was used to determine spotting efficiencies. After three washes to remove unbound detection antibodies, the slides were dried and scanned in a GenePix 4300A microarray scanner (Molecular Devices, San Diego, CA) for *M. tuberculosis* arrays or a GenePix 4000B for *M. avium* subsp. *paratuberculosis* arrays. Fluorescence intensity values for each spot were quantified using a GenePix 6.0 (Molecular Devices, Sunnyvale, CA) utilizing local background subtraction for each spot, and the data were exported in comma-separated-value (CSV) format. Each spot on the array is comprised of several hundred pixels. The raw values from array scans are median intensities of all the pixels in the printed spots after background subtraction for each protein or negative control.

Recombinant *M. avium* subsp. *paratuberculosis* antigen ELISA. Polysorb plates (Nunc; 96 well) were coated with 50 μl/well of 1 μg/ml recombinant *M. avium* subsp. *paratuberculosis* protein or MBP/LacZ or 5 μg/ml *M. avium* subsp. *paratuberculosis* total antigen sonicate extract in carbonate-bicarbonate buffer (0.06 M, pH 9.4). The plates were sealed and incubated overnight at 4°C and then

washed three times with 0.01 M PBS, pH 7.2, containing 0.05% Tween 20 (PBS-T) (Sigma-Aldrich, St. Louis, MO, USA). The wells were blocked by adding 200 μl/well of PBS-T containing 1% bovine serum albumin (PBS-T–BSA) and incubating at room temperature for 1 h before washing the plate three times with PBS-T. Serum samples, diluted 1:250 in PBS-T–BSA, were added to duplicate wells (100 μl/well) and incubated at room temperature for 1 h before washing three times with PBS-T. Then, 100 μl/well of anti-goat IgG peroxidase conjugate (Vector Laboratories, Burlingame, CA, USA) diluted 1:20,000 in PBS-T–BSA was added to all the wells and incubated at room temperature for 1 h before the plates were again washed three times with PBS-T. Finally, 100 μl/well of tetramethylbenzidine (TMB) SureBlue solution (KPL, Gaithersburg, MD, USA) was added, and the reaction was allowed to progress for 10 to 15 min at room temperature with no light before the reaction was stopped with 100 μl/well of TMB stop solution (KPL). Spectrophotometric reading of all the wells was performed at 450 nm using a SpectraMax 340PC384 microplate reader (Molecular Devices, Sunnyvale, CA, USA). Readings were analyzed by the S/P ratio, which was calculated as follows: S/P ratio = (sample OD − negative-control OD)/(positive-control OD − negative-control OD). Samples were considered positive if the S/P ratio was greater than 0.20.

Data analysis. The intensity data files in CSV format were read in, processed, and analyzed using an automated data analysis pipeline developed at ADI (Irvine, CA) that is implemented in R (http://www.r -project.org). Spot intensity measurements were converted into a single data matrix of intensities with the local background subtracted. For each sample, quality checks were performed for possible missing spots, contamination, and unusual background variation. The data were also inspected for the presence of subtle systematic effects and biases (probing day, slide, pad, print order, etc.). Once the data passed quality assurance, the final data set utilized for analysis was obtained by $\log_2$ transformation of raw intensities for variance stabilization without further adjustment due to low, homogeneous background levels. An antigen was classified as reactive to a given sample if antibody target signal intensity values were at least twice the sample's median IVTT negative control. Data were modeled using parametric (Student's t test) and nonparametric (Wilcoxon's rank sum test and area under the concentration-time curve [AUC] estimation) tests for between-group comparisons. The data were visualized using bar graphs, box plots, and heat maps for antibody levels. Hierarchical clustering of between-group antibody correlations was used to identify sets of antibody targets with diagnostic potential. Correlation of antibody responses between *M. avium* subsp. *paratuberculosis* and *M. tuberculosis* orthologs was assessed using Pearson's correlation coefficient (rho). Qualification of means was done, with 95% confidence intervals, and interquartile ranges were used for medians. P values were adjusted for the false-discovery rate (FDR) using the Benjamini-Hochberg method, and P values of <0.05 were considered significant (40).

SUPPLEMENTAL MATERIAL

Supplemental material for this article may be found at https://doi.org/10.1128/CVI .00081-17.

SUPPLEMENTAL FILE 1, PDF file, 3.4 MB.

ACKNOWLEDGMENTS

REFERENCES

1. Biet F, Boschiroli ML. 2014. Non-tuberculous mycobacterial infections of veterinary relevance. Res Vet Sci 97(Suppl):S69–S77. https://doi.org/10 .1016/j.rvsc.2014.08.007.
2. Bannantine JP, Paustian ML, Waters WR, Stabel JR, Palmer MV, Li L, Kapur V. 2008. Profiling bovine antibody responses to *Mycobacterium avium* subsp. *paratuberculosis* infection by using protein arrays. Infect Immun 76:739–749. https://doi.org/10.1128/IAI.00915-07.
3. Bannantine JP, Stabel JR, Bayles DO, Geisbrecht BV. 2010. Characteristics of an extensive *Mycobacterium avium* subspecies *paratuberculosis* recombinant protein set. Protein Expr Purif 72:223–233. https://doi.org/10 .1016/j.pep.2010.03.019.
4. Bannantine JP, Bayles DO, Waters WR, Palmer MV, Stabel JR, Paustian ML. 2008. Early antibody response against *Mycobacterium avium* subspecies *paratuberculosis* antigens in subclinical cattle. Proteome Sci 6:5. https:// doi.org/10.1186/1477-5956-6-5.
5. Kunnath-Velayudhan S, Salamon H, Wang HY, Davidow AL, Molina DM, Huynh VT, Cirillo DM, Michel G, Talbot EA, Perkins MD, Felgner PL, Liang X, Gennaro ML. 2010. Dynamic antibody responses to the *Mycobacte-*

rium tuberculosis proteome. Proc Natl Acad Sci U S A 107:14703–14708. https://doi.org/10.1073/pnas.1009080107.
6. Cayrou C, Turenne C, Behr MA, Drancourt M. 2010. Genotyping of *Mycobacterium avium* complex organisms using multispacer sequence typing. Microbiology 156:687–694. https://doi.org/10.1099/mic.0.033522-0.
7. Bannantine JP, Baechler E, Zhang Q, Li L, Kapur V. 2002. Genome scale comparison of *Mycobacterium avium* subsp. *paratuberculosis* with *Mycobacterium avium* subsp. *avium* reveals potential diagnostic sequences. J Clin Microbiol 40:1303–1310.
8. Bannantine JP, Zhang Q, Li LL, Kapur V. 2003. Genomic homogeneity between *Mycobacterium avium* subsp. *avium* and *Mycobacterium avium* subsp. *paratuberculosis* belies their divergent growth rates. BMC Microbiol 3:10. https://doi.org/10.1186/1471-2180-3-10.
9. Zakham F, Aouane O, Ussery D, Benjouad A, Ennaji MM. 2012. Computational genomics-proteomics and phylogeny analysis of twenty one mycobacterial genomes (tuberculosis and nontuberculosis strains). Microb Inform Exp 2:7. https://doi.org/10.1186/2042-5783-2-7.
10. Bannantine JP, Li L, Mwangi M, Cote R, Raygoza Garay JA, Kapur V. 2014.

Complete genome sequence of *Mycobacterium avium* subsp. *paratuberculosis*, isolated from human breast milk. Genome Announc 2:e01252-13. https://doi.org/10.1128/genomeA.01252-13.

11. Meena LS. 2015. An overview to understand the role of PE_PGRS family proteins in *Mycobacterium tuberculosis* H37 Rv and their potential as new drug targets. Biotechnol Appl Biochem 62:145–153. https://doi.org/10.1002/bab.1266.

12. Facciuolo A, Kelton DF, Mutharia LM. 2013. Novel secreted antigens of *Mycobacterium paratuberculosis* as serodiagnostic biomarkers for Johne's disease in cattle. Clin Vaccine Immunol 20:1783–1791. https://doi.org/10.1128/CVI.00380-13.

13. Souza GS, Rodrigues AB, Gioffre A, Romano MI, Carvalho EC, Ventura TL, Lasunskaia EB. 2011. Apa antigen of *Mycobacterium avium* subsp. *paratuberculosis* as a target for species-specific immunodetection of the bacteria in infected tissues of cattle with paratuberculosis. Vet Immunol Immunopathol 143:75–82. https://doi.org/10.1016/j.vetimm.2011.06.026.

14. Cho D, Sung N, Collins MT. 2006. Identification of proteins of potential diagnostic value for bovine paratuberculosis. Proteomics 6:5785–5794. https://doi.org/10.1002/pmic.200600207.

15. Cho D, Shin SJ, Talaat AM, Collins MT. 2007. Cloning, expression, purification and serodiagnostic evaluation of fourteen *Mycobacterium paratuberculosis* proteins. Protein Expr Purif 53:411–420. https://doi.org/10.1016/j.pep.2006.12.022.

16. Willemsen PT, Westerveen J, Dinkla A, Bakker D, van Zijderveld FG, Thole JE. 2006. Secreted antigens of *Mycobacterium avium* subspecies *paratuberculosis* as prominent immune targets. Vet Microbiol 114:337–344. https://doi.org/10.1016/j.vetmic.2005.12.005.

17. Li L, Munir S, Bannantine JP, Sreevatsan S, Kanjilal S, Kapur V. 2007. Rapid expression of *Mycobacterium avium* subsp. *paratuberculosis* recombinant proteins for antigen discovery. Clin Vaccine Immunol 14:102–105. https://doi.org/10.1128/CVI.00138-06.

18. Paustian ML, Kapur V, Bannantine JP. 2005. Comparative genomic hybridizations reveal genetic regions within the *Mycobacterium avium* complex that are divergent from *Mycobacterium avium* subsp. *paratuberculosis* isolates. J Bacteriol 187:2406–2415. https://doi.org/10.1128/JB.187.7.2406-2415.2005.

19. Semret M, Alexander DC, Turenne CY, de Haas P, Overduin P, van Soolingen D, Cousins D, Behr MA. 2005. Genomic polymorphisms for *Mycobacterium avium* subsp. *paratuberculosis* diagnostics. J Clin Microbiol 43:3704–3712. https://doi.org/10.1128/JCM.43.8.3704-3712.2005.

20. Leite FL, Reinhardt TA, Bannantine JP, Stabel JR. 2015. Envelope protein complexes of *Mycobacterium avium* subsp. *paratuberculosis* and their antigenicity. Vet Microbiol 175:275–285. https://doi.org/10.1016/j.vetmic.2014.11.009.

21. Bannantine JP, Huntley JF, Miltner E, Stabel JR, Bermudez LE. 2003. The *Mycobacterium avium* subsp. *paratuberculosis* 35 kDa protein plays a role in invasion of bovine epithelial cells. Microbiology 149:2061–2069. https://doi.org/10.1099/mic.0.26323-0.

22. Bannantine JP, Lingle CK, Stabel JR, Ramyar KX, Garcia BL, Raeber AJ, Schacher P, Kapur V, Geisbrecht BV. 2012. MAP1272c encodes an NlpC/P60 protein, an antigen detected in cattle with Johne's disease. Clin Vaccine Immunol 19:1083–1092. https://doi.org/10.1128/CVI.00195-12.

23. Schiller I, Oesch B, Vordermeier HM, Palmer MV, Harris BN, Orloski KA, Buddle BM, Thacker TC, Lyashchenko KP, Waters WR. 2010. Bovine tuberculosis: a review of current and emerging diagnostic techniques in view of their relevance for disease control and eradication. Transbound Emerg Dis 57:205–220. https://doi.org/10.1111/j.1865-1682.2010.01148.x.

24. More SJ, Radunz B, Glanville RJ. 2015. Lessons learned during the successful eradication of bovine tuberculosis from Australia. Vet Rec 177:224–232. https://doi.org/10.1136/vr.103163.

25. O'Brien DJ, Schmitt SM, Fitzgerald SD, Berry DE. 2011. Management of bovine tuberculosis in Michigan wildlife: current status and near term prospects. Vet Microbiol 151:179–187. https://doi.org/10.1016/j.vetmic.2011.02.042.

26. Coad M, Clifford DJ, Vordermeier HM, Whelan AO. 2013. The consequences of vaccination with the Johne's disease vaccine, Gudair, on diagnosis of bovine tuberculosis. Vet Rec 172:266. https://doi.org/10.1136/vr.101201.

27. Fitzgerald SD, Bolin SR, Boland KG, Lim A, Kaneene JB. 2011. Overt *Mycobacterium avium* subsp. *paratuberculosis* infection: an infrequent occurrence in archived tissue from false TB reactor cattle in Michigan, USA. Vet Med Int 2011:910738. https://doi.org/10.4061/2011/910738.

28. Stabel JR. 2000. Transitions in immune responses to *Mycobacterium paratuberculosis*. Vet Microbiol 77:465–473. https://doi.org/10.1016/S0378-1135(00)00331-X.

29. Wang C, Turnbull BW, Grohn YT, Nielsen SS. 2006. Estimating receiver operating characteristic curves with covariates when there is no perfect reference test for diagnosis of Johne's disease. J Dairy Sci 89:3038–3046. https://doi.org/10.3168/jds.S0022-0302(06)72577-2.

30. Wang C, Turnbull BW, Nielsen SS, Grohn YT. 2011. Bayesian analysis of longitudinal Johne's disease diagnostic data without a gold standard test. J Dairy Sci 94:2320–2328. https://doi.org/10.3168/jds.2010-3675.

31. Wagner B, Freer H, Rollins A, Erb HN, Lu Z, Grohn Y. 2011. Development of a multiplex assay for the detection of antibodies to *Borrelia burgdorferi* in horses and its validation using Bayesian and conventional statistical methods. Vet Immunol Immunopathol 144:374–381. https://doi.org/10.1016/j.vetimm.2011.08.005.

32. Janagama HK, Kumar S, Bannantine JP, Kugadas A, Jagtap P, Higgins L, Witthuhn B, Sreevatsan S. 2010. Iron-sparing response of *Mycobacterium avium* subsp. *paratuberculosis* is strain dependent. BMC Microbiol 10:268. https://doi.org/10.1186/1471-2180-10-268.

33. Bull TJ, Linedale R, Hinds J, Hermon-Taylor J. 2009. A rhodanine agent active against non-replicating intracellular *Mycobacterium avium* subspecies *paratuberculosis*. Gut Pathog 1:25. https://doi.org/10.1186/1757-4749-1-25.

34. Lee JS, Shin SJ, Collins MT, Jung ID, Jeong YI, Lee CM, Shin YK, Kim D, Park YM. 2009. *Mycobacterium avium* subsp. *paratuberculosis* fibronectin attachment protein activates dendritic cells and induces a Th1 polarization. Infect Immun 77:2979–2988. https://doi.org/10.1128/IAI.01411-08.

35. Liang L, Leng D, Burk C, Nakajima-Sasaki R, Kayala MA, Atluri VL, Pablo J, Unal B, Ficht TA, Gotuzzo E, Saito M, Morrow WJ, Liang X, Baldi P, Gilman RH, Vinetz JM, Tsolis RM, Felgner PL. 2010. Large scale immune profiling of infected humans and goats reveals differential recognition of *Brucella melitensis* antigens. PLoS Negl Trop Dis 4:e673. https://doi.org/10.1371/journal.pntd.0000673.

36. Felgner PL, Roestenberg M, Liang L, Hung C, Jain A, Pablo J, Nakajima-Sasaki R, Molina D, Teelen K, Hermsen CC, Sauerwein R. 2013. Pre-erythrocytic antibody profiles induced by controlled human malaria infections in healthy volunteers under chloroquine prophylaxis. Sci Rep 3:3549. https://doi.org/10.1038/srep03549.

37. Kunnath-Velayudhan S, Davidow AL, Wang HY, Molina DM, Huynh VT, Salamon H, Pine R, Michel G, Perkins MD, Xiaowu L, Felgner PL, Flynn JL, Catanzaro A, Gennaro ML. 2012. Proteome-scale antibody responses and outcome of *Mycobacterium tuberculosis* infection in nonhuman primates and in tuberculosis patients. J Infect Dis 206:697–705. https://doi.org/10.1093/infdis/jis421.

38. Bannantine JP, Paustian ML. 2006. Identification of diagnostic proteins in *Mycobacterium avium* subspecies *paratuberculosis* by a whole genome analysis approach. Methods Mol Biol 345:185–196.

39. Zhu H, Snyder M. 2003. Protein chip technology. Curr Opin Chem Biol 7:55–63. https://doi.org/10.1016/S1367-5931(02)00005-4.

40. Benjamini Y, Hockberg Y. 1995. Controlling the false discovery rate: a practical and powerful approach to multiple testing. J R Stat Soc B 57:289–300.

41. Hughes V, Bannantine JP, Denham S, Smith S, Garcia-Sanchez A, Sales J, Paustian ML, McLean K, Stevenson K. 2008. Immunogenicity of proteome-determined *Mycobacterium avium* subsp. *paratuberculosis*-specific proteins in sheep with paratuberculosis. Clin Vaccine Immunol 15:1824–1833. https://doi.org/10.1128/CVI.00099-08.

42. Gurung RB, Begg DJ, Purdie AC, Bannantine JP, Whittington RJ. 2013. Antigenicity of recombinant maltose binding protein-*Mycobacterium avium* subsp. *paratuberculosis* fusion proteins with and without factor Xa cleaving. Clin Vaccine Immunol 20:1817–1826. https://doi.org/10.1128/CVI.00596-13.

43. Leroy B, Roupie V, Noel-Georis I, Rosseels V, Walravens K, Govaerts M, Huygen K, Wattiez R. 2007. Antigen discovery: a postgenomic approach to paratuberculosis diagnosis. Proteomics 7:1164–1176. https://doi.org/10.1002/pmic.200600988.